

The *gem*-dimethyl effect in reactions through tetrahedral intermediates: cyclizations of some ethyl 2,3-disubstituted-5-(*p*-nitrophenyl) hydantoates

Asen H. Koedjиков, Petko M. Ivanov, and Ivan G. Pojarlieff*

Institute of Organic Chemistry, Bulgarian Academy of Sciences, ul. Acad. G. Bonchev block 9,
Sofia 1113, Bulgaria

E-mail: ipojarli@orgchm.bas.bg

Dedicated to Professor Oswald Tee on the occasion of his 60th birthday
(received 13 Sep 01; accepted 25 Oct 01; published on the web 02 Nov 01)

Abstract

The kinetics of cyclization for 3-ethyl-, 3-isopropyl- and 3-hexyl-substituted hydantoates **2-UE** to the corresponding hydantoins **2-Hyd** were studied in an attempt to examine the *gem*-dimethyl effect (GDME) in a case where the tetrahedral center of the intermediate **T** is not fully screened. However, in these congested compounds, the increase in strain in the open chains paralleled that of the intermediates resulting in meager rate enhancements – an interpretation confirmed by MM3 calculations. In the case of the largest substituent **2d-UE** a new reaction appeared in the rate profile, together with substantial changes concerning the points of transition from r.d. formation to breakdown of **T** in the OH⁻ and general base catalysis. All these agree with the concept that the GDME tends to shift the transition state to an earlier step of the cyclization reaction.

Keywords: Hydantoates, cyclicizations, tetrahedral intermediates, *gem*-dimethyl effect

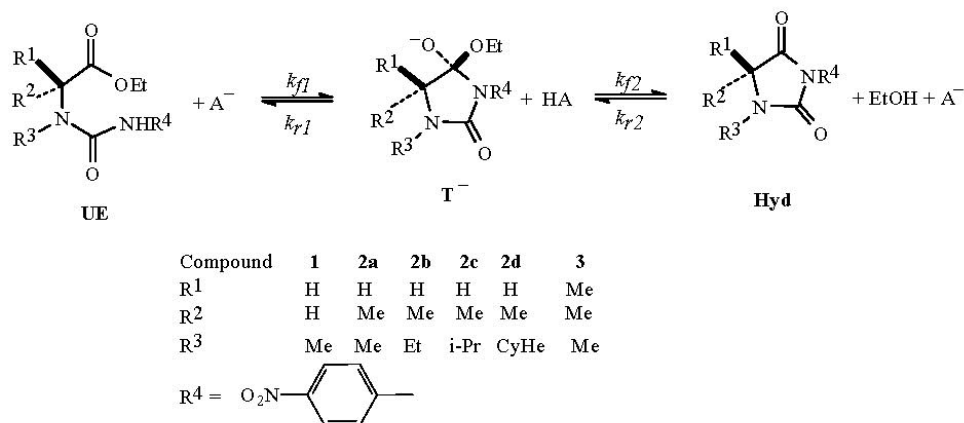
Introduction

The *gem*-dimethyl effect¹, GDME, *i.e.* the acceleration of cyclization reactions by substituents in the chain, is a convenient means of designing bioorganic substrates because of the expected minor perturbations in reactivity. Sometimes, however, substituents may slow down the reaction instead of making it faster and worse, as far as models are concerned, cause a change in mechanism. Often the reasons for the retardation are trivial and can be traced to steric hindrance. Recently, we observed^{2,3} loss of the GDME in the base-catalyzed cyclization of ethyl hydantoates when all hydrogens are replaced by methyl groups accompanied by a change in the mechanism. The role of steric repulsions in the tetrahedral intermediate was excluded because the acid-catalyzed cyclization showed a normal GDME. The case of ethyl 5-(*p*-nitrophenyl)-

hydantoates (**UE**) was particularly intriguing since these compounds exhibited complex pH-rate profiles and that of the trimethylated ester **3-UE** was distinctly different showing a loss of the GDME for OH⁻ catalysis and changes in mechanism both for acid and for base catalysis. The variation in rate and mechanism with the introduction of methyl groups in the chain could be explained by the interplay of two factors:

(a) The GDME eases cyclization but hinders ring-opening. This results from strain in the open compound being relieved in the ring because the bonds forming the cycle are forced into unfavourable conformations thus leaving more freedom for the substituents. In cyclizations through tetrahedral intermediates⁴ giving rigid products such as hydantoin flexibility is gradually lost along the reaction path and the GDME will influence both steps of Scheme 1. If k_{f2} is rate determining the GDME can shift the overall transition state towards the first stage, k_{f1} , by making $k_{r1} < k_{f2}$.

(b) Steric hindrance to proton transfer to the departing ethoxy anion in the permethylated intermediate **3-T** which contrarily makes the second stage, k_{f2} , slow in the base-catalyzed reaction. The latter hindrance arises in the ring intermediate because the oxygen atom of the ethoxy group is flanked by the *gem*-dimethyl group on one side and the substituent R³ on 1-N on the other while a frontal approach is made difficult by the ethyl group. In the 5-(*p*-nitrophenyl)hydantoates² and related cases³ the change in mechanism is accompanied by a loss of the GDME because the proton transfer step has become more slow than the cyclization step forming **T**⁻.



Scheme 1

In order to distinguish more clearly the two effects we studied molecules where increase in strain was not expected to change the immediate environment of the reacting groups and thus elucidate the action of the *gem*-dimethyl effect “itself”. The cyclization of esters **2b**-, **2c**- and **2d-UE**, reported in this paper, is just such a case where strain is introduced by increasing the size of the substituent on 3-N (1-N in the product hydantoin), a position removed by one atom from both the ester and the attacking nitrogen atom.

Results and Discussion

a) The pH-rate profiles and mechanisms

The rates of cyclizations of 3-substituted ethyl 5-(4-nitrophenyl)hydantoates to hydantoins were found rather insensitive to the substitution of methyl for ethyl and even for isopropyl as can be seen on Fig. 1.[§] Acid catalysis, k_{IH} in Table 1, is increased only by a factor of 2, while the increase of k_{OH}^b (alkaline catalysis, see below) is even more modest. This contrasts the effect of the same series of 1'-N-substituents in the cyclization of ureidosuccinic acids in KOH where substitution of Me for cyclohexyl brought about an acceleration of ca. 20 times.⁵ The meager enhancement of cyclization rate of the esters described in this paper could be due to buttressing of 2-methyl by the N-substituent increasing the strain in the sterically more demanding transition state of the esters thus offsetting the GDME. The compound with greatest size of the N-substituent, **2d-UE**, shows however some considerable changes in the form of the rate profile. Esters **2b-UE** and **2cUE** repeat the pH-rate profile of **2a-UE** (Figure 1) characterized by two regions of negatively charged transition state separated by a poorly expressed plateau of charge zero. When Me is replaced by cyclohexyl (Figure 2), the rate profile begins to resemble that of hydantoate **3-UE** carrying the maximum of three methyl groups in the chain.

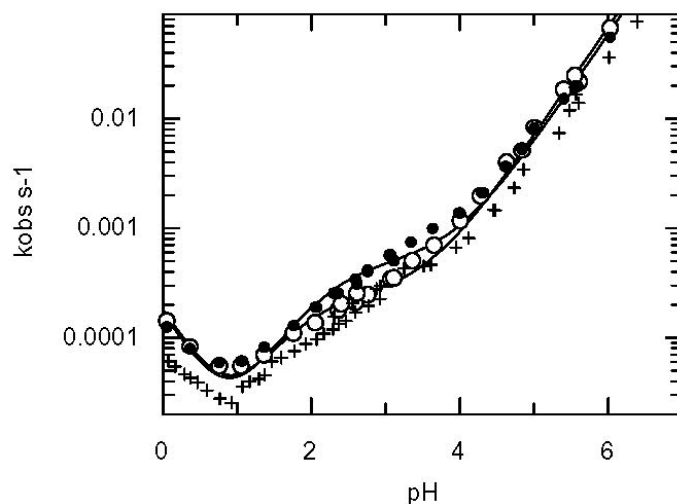


Figure 1 Semilogarithmic plot of the pseudo first order rate constants against pH. **2b-UE** -closed circles; **2c-UE** – open circles. For comparison x present data for **2a-UE**.² Lines drawn by means of eqn. (2) and parameters from Table 1.

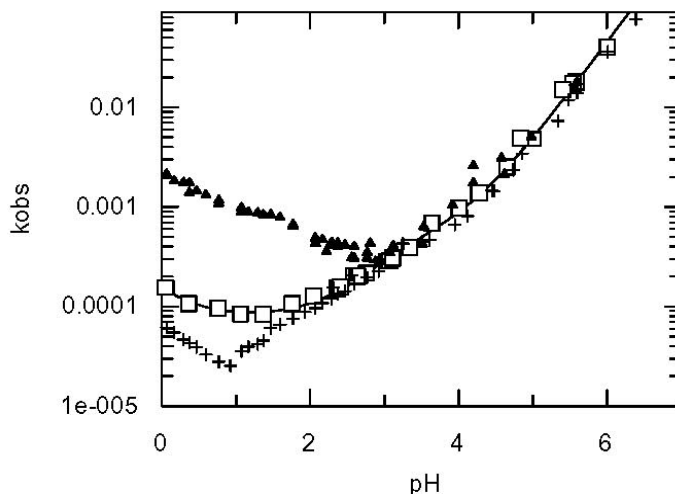


Figure 2 Semilogarithmic plot of the pseudo first order rate constants against pH. **2d-UE** open squares; **2a-UE** +; **3-UE** closed triangles. Line drawn by means of eqn. (4) and parameters for **2d-UE** from Table 1.

The new features in the rate profile of **2d-UE** is the appearance of a second “neutral” reaction below pH 2 and closing of the difference in the rates of the two OH⁻ reactions; in ester **3-UE** there is actually a single OH⁻ reaction. The behaviour in buffers, to be discussed below, is also different.

In order to understand the difference in the shape of the profiles on Fig. 1 and 2 we need to recall the main features of our interpretation of the kinetics of cyclization of methyl-substituted 5-(p-nitrophenyl)-hydantoates.² In the case of **1-UE** and **2a-UE** the two *ba* reactions catalyzed by OH⁻ can be denoted for simplicity as k_{OH}^b at high pH and k_{OH}^a at low pH. Actually according to the preferred mechanism k_{OH}^a results from an inverse proportionality in a_H in eqn (1) used to describe the pH-rate profile.

$$k_{obs} = k_{1H}a_H + \frac{k_w + k_{OH}^b a_{OH}}{1 + k_{2H}a_H} \quad (1)$$

Acid catalysis k_{1H} is treated as a separate reaction while the fractional term of eqn. (1) is derived from the steady-state solution of Scheme 1 ($A^- = H_2O$ or OH^-), eqn. (2)

$$k_{obs} = \frac{(k_{f1w} + k_{f1OH}a_{OH})(k_{f2w} + k_{f2H}a_H)}{k_{r1w} + k_{f2w} + (k_{r1H} + k_{f2H})a_H} \quad (2)$$

by implementing the conditions $k_{r1w} < k_{f2w}$ for the water-catalyzed partitioning of the intermediate T^- and $k_{r1H} > k_{f2H}$ for the H^+ -catalyzed partitioning from mechanistic considerations discussed in ref.2 and imposing some limitations on the relative size of the constants of the elementary steps.

In eqn (1) $k_{OH}^b = k_{f1OH}$, $k_w^b = k_{f1w}$, $k_{2H} = k_{r1H} / k_{f2w}$ and $k_{OH}^a = k_w^b / k_{2H}K_w$.

Mechanistically, k_{OH}^b is a specific base catalyzed attack of the ureide anion. At low pH the breakdown of T^- to reactants catalyzed by H^+ is faster than that to products, that is formation of T^- becomes an equilibrium, and k_{OH}^a presents acid inhibition⁶ of T^- . In this pH region

$$k_{obs} = k_{OH}^a a_{OH} = \frac{k_{f1w} k_{f2w}}{k_{r1H} a_H} = \frac{K_T}{K_w} k_{f2w} a_{OH} \quad (3)$$

where K_T is the equilibrium constant of the first reaction of Scheme 1 when A^- is water and AH is hydroxonium ion.

As demonstrated on Fig. 1, eqn. (1) gave a fully satisfactory fit to the rate data the newly studied *N*-ethyl and *N*-isopropyl derivatives **2b-UE** and **2c-UE**. The appearance of a second plateau at low pH, k_w^a with the cyclohexyl compound **2d-UE** is not provided for by eqn. (1) because it has been derived on the assumption that in eqn. (2) the condition $k_{f2w} > k_{f2H} a_H$ holds throughout the pH interval studied. When this restriction is removed eqn. (4) obtains which gives a good fit to the rate data for **2d-UE** (Fig. 2):

$$k_{obs} = \frac{(k_w^b + k_{OH}^a a_{OH})(1 + k_{3H}^a a_H)}{1 + k_{2H}^a a_H} + k_{1H}^a a_H \quad (4)$$

where $k_{3H} = k_{f2H} / k_{f2w}$ (because $k_{r1w} < k_{f2w}$). Eqn (4) shows readily that the rate at the plateau at lower pH then becomes

$$k_w^a = k_w^b k_{3H} / k_{2H} = k_{f1w} k_{f2H} / k_{r1H} = K_T k_{f2H} \quad (5)$$

The rate constants obtained from non-linear regression fits of the rate data to eqns (1 and (4) are listed in Table 1.

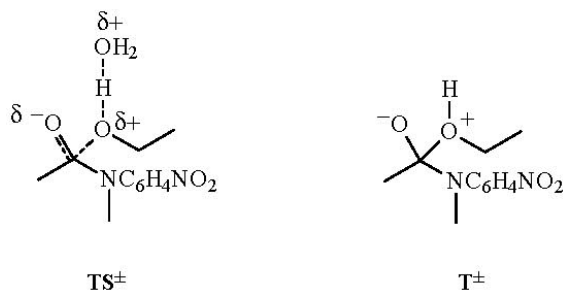
Table 1 Rates of cyclization of ethyl 2-methyl-3-alkyl-5-p-nitrophenylhydantoates in water at 25.0 °C and ionic strength 1 M (KCl)

Ureido ester	$10^4 k_{1H}$ dm ³ mol ⁻¹ s ⁻¹	$10^{-6} k_{OH}^b$ dm ³ mol ⁻¹ s ⁻¹	$10^4 k_w^b$ s ⁻¹	$10^{-2} k_{2H}$ dm ³ mol ⁻¹ s ⁻¹	$10^{-8} k_{OH}^a$ dm ³ mol ⁻¹ s ⁻¹
2a-UE ^{b,c}	0.834±0.061	3.85±0.20	2.18±0.16	1.07±0.16	2.07
2b-UE ^b	1.65±0.19	5.90 ± 0.38	4.90 ± 0.50	1.66 ± 0.34	2.95
2c-UE ^b	1.77±0.17	6.88 ± 0.34	2.51 ± 0.20	0.783 ± 0.151	3.19
2d-UE ^{d,e,f}	0.781±0.20	4.49 ± 0.22	5.56 ^e ± 1.07	15.7 ± 5.6	0.353

^a $k_w^b / k_{2H} K_w$. ^b From a fit to eqn. (1). ^c From ref. 2. ^d From a fit to eqn. (4). ^e $k_w^a = k_w^b k_{3H} / k_{2H} = 7.8 \times 10^{-5}$

s⁻¹. ^f $k_{3H} = 220 \pm 52$

Thus according to eqn. (5), the second pH independent region at lower pH is due to rate limiting reaction of \mathbf{T}^- with \mathbf{H}^+ .



A concerted mechanism corresponding to the transition state, \mathbf{TS} , has been preferred for the reaction presented by k_{OH}^a where, however, the acid is a molecule of water.^{2,3,7†} The protonation by $\mathbf{H}_3\text{O}^+$ leading to \mathbf{T}^\pm should be an energetically downhill reaction; so that protonation and breakdown of the tetrahedral intermediate could be consecutive processes.

This analysis affords also a mechanistic interpretation of the rate profile of ester **3UE** studied before² (Fig.2). Two zones of slope zero were identified centered roughly at pH 3 and 1.5, respectively, separated by a slope of minus 1. Up to the highest pH studied there is a single base-catalyzed reaction (slope of plus 1) assigned as cleaving of EtO from **3-T** generally acid catalyzed by water the same as k_{OH}^a in the profiles of esters **2-UE** shown on Fig. 1. Thus in the pH-region of transition from slope 1 to 0, \mathbf{T} is equilibrating with the reactants, so that the plateau at higher pH could be either breakdown of the neutral \mathbf{T}^0 or, more likely, the kinetically equivalent reaction of \mathbf{T}^- with \mathbf{H}^+ . The latter preference is now reinforced because eqns. (4) and (5) appear to be reasonable extensions of the behaviour of \mathbf{T}^- of the 5-p-nitrophenyl esters.

What causes the appearance of the reaction designated as k_w^a in the case of hydantoates **2d-UE**? In terms of the derivation of eqn. (1) from eqn. (2) this is because below a certain pH (2 with **2d-UE**) the inequality $k_{f2w} > k_{f2HAH}$ changes to $k_{f2w} < k_{f2HAH}$ leading to eqn. (4), *i.e.* the rate constant for acid catalyzed breakdown of \mathbf{T} increases compared to the constant for water catalysis. As discussed in the Introduction under (a) the GDME accelerates the forward steps so that the increase in k_{f2} is wholly expected, what is not immediately obvious is why the increase is less for water catalysis in order for the inequality $k_{f2w} > k_{f2HAH}$ to change sign in the same pH region. Actually for the cyclohexyl derivative the value for $k_{2H} = k_{r1H} / k_{f2w}$ is substantially greater than that for the remaining compounds while the value for $k_{OH}^a = \frac{K_{T^-}}{K_w} k_{f2w}$ is substantially lower (Table 1). These values indicate that k_{f2w} is smaller with the cyclohexyl derivative than with the other ones thus contributing to the appearance of the k_w^a reaction.[‡] The appearance of same reaction in the case of **3-UE** with an obviously stronger GDME at pH ca. 3 is on the other hand an indication of the role of a relative increase of k_{f2H} .

The second phenomenon observed with the cyclohexyl derivative **2d-UE** is that k_w^a and k_{OH}^b become close in value; the ratio k_w^a / k_{OH}^b is about 50 for compounds **2a-2c-UE** but only 8 for **2d-**

UE (as a result the plateau at higher pH is hardly discerned). Thus the profile of **2d-UE** is midway between those of ester **3-UE**² and its acid⁸ with a single OH⁻ catalyzed reaction and the profiles of esters **2a-c-UE** and the acid of **2a-UE** exhibiting two OH⁻ catalyzed reactions.* This can be understood in terms of the conditions necessary to observe two reactions catalyzed by the same species:⁹ there should be two different modes for partitioning of the intermediate caused by differences in the partitioning ratio k_{f2} / k_{r1} (in practice < 1 or > 1).⁹ And secondly, the intermediate should not be in equilibrium with the reagents at least in one of the modes. Relevant for comparison is the free acid of **3-UE** because when the ethyl group in the ester is replaced by hydrogen no steric hindrance to protonation comes into play (paragraph (b) in the Introduction). The mechanism for OH⁻ catalysis with the acid** could readily be assigned as that of k_{OH}^b of the less substituted esters and acids: slow formation of **T** by attack of the preliminary ionized ω -(p-nitrophenyl)ureido group. This mechanism demands $k_{f2w} / k_{r1w} > 1$ as can be readily seen from eqn. (2) for the first step to be rate-determining at high pH. With the less substituted compounds a change of mechanism occurs at lower pH because $k_{f2H} / k_{r1H} < 1$. The loss of the second reaction at lower pH in the case of the free acid of **3-UE** was attributed to the GDME enhancing the rate in the forward direction and decreasing it in the reverse. This overturns the ratio k_{f2H} / k_{r1H} to greater than unity so that no change in mechanism can be observed. Apparently the presently studied cyclohexyl ester **2d** is somewhere in between the free acids of **2a-UE** and **3-UE**: the two OH⁻ reactions are still discernible but the difference is strongly diminished manifesting the action of the GDME.

(b) Buffer catalysis

The compounds studied showed buffer catalysis which could be identified as general base catalysis, GBC. The results obtained are summarized in Table 2.

Table 2 Buffer catalysis data for the cyclization of 3-substituted ethyl 5-(4-nitrophenyl)-2-methylhydantoates at 25 °C and ionic strength 1.0 M

Buffer acid	pK _{AH} ^a	Conc. range mol dm ⁻³	% base	10 ⁴ k _B , k _{BH} in parenthesis dm ³ mol ⁻¹ s ⁻¹ , ^b		
				2b	2c	2d
H ₃ N ⁺ CH ₂ CO ₂ H	2.45	0.05-1	30	9.11±2.13	25.2±3.3	38.8±0.3.1
		0.05-0.2	50		(3.42±0.78)	
		0.05-0.2	70			
HCO ₂ H	3.57	0.01-0.2	30	251±43	203±28	118±5
		0.01-0.2	50	(6.39±2.54)	(5.00±1.94)	
		0.01-0.2	70			
CH ₃ CO ₂ H	4.62	0.01-0.2	30	1190±160	1090±150	465±32
		0.01-0.2	50	(6.07±2.04)	(2.79±1.68)	
		0.01-0.2	70			
		0.05-0.2	90			
(CH ₃)AsO ₂ H	6.19	0.01-0.15	10	3400±380	4410±630	3990±360
		0.01-0.15	20			
		0.01-0.15	30			
H ₂ PO ₄ ⁻	6.48	0.032-0.2	10	4860±120	8890±120	4140±1070

^apK_{AH}-values from ref. 10. ^bWhen no k_{BH} is presented k_B results from fitting to eqn. (6), when both constants are presented these have been obtained by means of eqn. (7).

The procedures followed have been described in ref. 2. In cases of uncomplicated GBC plots of k_{buf} (the slopes of k_{obs} against buffer concentration at constant buffer ratio) against fraction base are straight lines with slopes equal to k_B , the rate constant for catalysis by the general base B. Often upward curvatures in such plots have been observed before in the cyclization of ureido esters and acids and can be due to various reasons.^{2, 3, 8} This is related to an important difference between the cyclohexyl derivative **2d-UE** and the remaining esters **2a-c-UE** demonstrated on Figure 3. The plot for the former is a straight line in acetate buffers while the rest are curved upward. The slope of the straight line, k_B for acetate anion, is 0.046 ± 0.009 , the same value as that shown on Table 2 which has been obtained by simultaneous fitting of all data by a non-linear regression

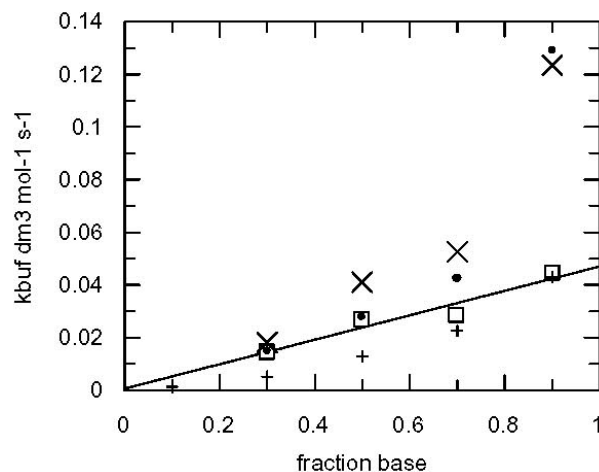


Figure 3. Plots of k_{buf} against fraction base in acetate buffers for esters **2a-UE** – +, **2b-UE** – full circles, **2c-UE** – X, **2d-UE** – open squares. The line presents a linear fit to the data for **2d-UE**.

With esters such as the N-methyl derivative **2a-UE** the curvature is due to a change in mechanism.² The GBC has been assigned to k_{f1} and a transition takes place similar to that k_{OH}^b to k_w^a when the pH is lowered *i.e.* first stage on Scheme 1 becomes a preliminary equilibrium when $k_{r1AH}a_H > k_{f2w}^{**}$. The mechanism of the GBC reaction changes when the breakdown to reactants catalyzed by the general acid AH becomes faster than the breakdown to products $k_{r1AH} [AH] > k_{f2w}$.

The conditions for the latter transition can be readily appreciated from the above discussion of the rate equations. Above pH 3-4 the hydantoates cyclize by rate-determining formation of T^- .[♦] Since the catalysis by the general base has to take place in the rate-determining stage of the main reaction in this region, simple GBC as observed in acetate for **2d-UE** can result from two simultaneous conditions when the terms for catalysis by the general base A^- are included in eqn. (1): $k_{f2w} > k_{f2AH}[AH]$ in the numerator and $k_{r1AH}[AH] < k_{f2w}$ in the denominator.[♦] Then eqn. (1) can be expanded as

$$k_{obs} = \frac{k_w + k_{OH}a_{OH} + k_B [A^-]}{1 + k_{2H}a_H} + k_{1H}a_H \quad (6)$$

where $k_B = k_{f1A^-}$ of eqn. (2). When at higher $[AH]$ $k_{r1AH}[AH] > k_{f2w}$ we obtain

$$k_{obs} = \frac{k_w + k_{OH} \alpha_{OH} + k_B [A^-]}{1 + k_{2H} \alpha_H + k_{BH} [AH]} + k_{1H} \alpha_H \quad (7)$$

where $k_{BH} = k_{r1AH} / k_{f2w}$. At sufficiently large $[AH]$ the contribution of buffer catalysis becomes equal to the rate described by eqn. (3), *i.e.* r.d. breakdown of T^- catalyzed by water. In the case of **2d-UE** for buffers more acidic than acetate the k_B and k_{BH} terms were added to eqn. (4) as above. The collected k_{obs} data for each buffer were fitted both to the equation with and without a k_{BH} term in the denominator and the better fits are given in Table 2.

Why does the k_{BH} term disappear in the case of the cyclohexyl derivative **2d-UE** in acetate and more acidic buffers? This is another phenomenon in line with the GDME upon partitioning of tetrahedral intermediates. The k_{BH} term being equal to k_{r1AH} / k_{f2w} should decrease with the GDME because the latter decreases k_{r1} and increases k_{f2} . Apparently, k_{BH} with **2d-UE** is too small to cause a shift in the rate determining step.

The GBC catalysis has been assigned² to removal of the ω -N-H proton concerted with the formation of T^- . Fig. 4 illustrates the similarity of the Brønsted plots of compounds

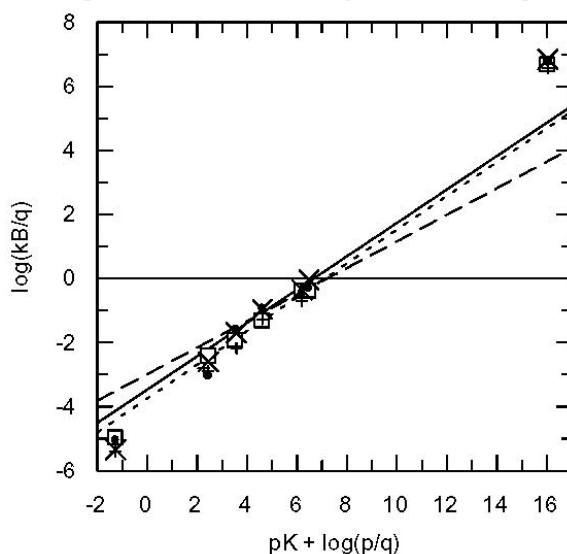


Figure 3 Brønsted plots of rate constants for GBC (p and q are statistical corrections for number of protons and basic sites respectively). Cyclization of **2a-UE** – +, **2b-UE** – full circles, **2c-UE** – X, and **2d-UE** – open squares. Lines are linear fits to 4 points from formate to phosphate for **2b-UE** (dashes) and **2c-UE** (unbroken line), and fit to 5 points from glycine to phosphate for **2d-UE** (dots)

2b – **2d-UE** to that of the *N*-methyl derivative **2a-UE** studied before² The points for catalysis by water and hydroxide deviate and were excluded in the calculation of the Brønsted β -values listed

on Table 3. For compounds **1-UE** and **2-UE** these are around 0.50 ± 0.08 . All this adds further credence on the above interpretations based on the presumption that the same mechanism operates.*.

Table 3. Brønsted β -values for general base catalysis of the cyclization of ethyl p-nitrophenylhydantoates

Compound	β	# of points	r
1-UE	0.50a	5	0.9559
2a-UE	0.58a	5	0.9866
2b-UE	0.42	4a	0.9834
2c-UE	0.525	4	0.9902
2d-UE	0.53	5	0.9975

^a From ref. 2.

(c) *Steric strain*

As pointed out already, unexpectedly no significant rate increase of cyclization was observed with increasing the size of the 1'-N-substituent. There is little doubt that the source of the GDME – the strain in the open-chained esters increases in the series **2a-UE** – **2d-UE**. One albeit indirect indication are the NMR signals for CH₂ of the ester ethyl groups (Table 5). At the resolution used diastereotopicity showed up only with the isopropyl and cyclohexyl derivatives indicating conformational restriction. In order to check the hypothesis that the strain increases to a similar degree in the transition state molecular mechanics and semi empirical calculations were carried out on the esters and on the tetrahedral intermediates **T⁻** (Scheme 1). The molecular mechanics modeling was carried out utilizing the MM3 force field.¹⁴ A partial atomic charge -0.6 was placed on the O-atom of the tetrahedral intermediates as determined from AM1 computations. An effective dielectric constant 2.0 was used for the estimation of the electrostatic interactions. MOPAC 93.00 was used for the semiempirical molecular orbital calculations.¹⁵

Examination of the structural parameters (torsional and bond angles) obtained by means of MM3 could not pin-point to any drastic changes brought about by the Ncyclohexyl group. One significant feature is however the marked decreased puckering of the ring in **T⁻** of **2d-UE** accompanied by broadening of the endo bond angles. Apparently the ring is in some way compressed in spite of being equatorial in the cyclohexane ring according to the proton couplings in the NMR. The strain energies cannot be compared directly because the compounds carry different number of atoms. This is circumvented by comparing the double differences:

$$\begin{aligned} \Delta\Delta\text{Strain} &= \Delta\text{StrainT}^- - \Delta\text{Strain}_{\text{Hyd}} \\ \Delta\text{Strain} &= \text{Strain}(\mathbf{n}) - \text{Strain}(\mathbf{1}), \mathbf{n} = \mathbf{1}, \mathbf{2a}, \mathbf{2d}, \mathbf{3} \end{aligned} \quad (8)$$

Table 4. MM3 strain energies^a

Compound	$\Delta\text{StrainT} - \Delta\text{StrainHyd}$	$\Delta\Delta\text{Strain}$
1	$(6.7 - 6.7) - (19.9 - 19.9) = 0.0 - 0.0$	$= 0.0$
2a	$(9.8 - 6.7) - (22.9 - 19.9) = 3.1 - 3.0$	$= 0.1$
2d	$(13.0 - 6.7) - (26.4 - 19.9) = 6.3 - 6.5$	$= 0.2$
3	$(11.6 - 6.7) - (27.7 - 19.9) = 4.9 - 7.8$	$= 2.9$

^a Details from the calculations are available on request from the authors.

The data in the second column of Table 4 nicely confirm the assumption that the practical absence of rate increase upon enlarging the 3-N-substituent in the hydantoates is due to parallel increase in the cyclic transition state. In compound **3-UE** which shows a normal GDME (Fig. 2) the double difference is decreased in the absolute sense because of the larger strain in the open chain as demanded by theory.

Conclusions

The behaviour of ethyl 3-cyclohexyl-2-methylhydantoate, **2d-UE**, compared to that of the esters with smaller substituents in position 3 is characterized by the appearance of a new reaction, decreased difference in the rates of the two OH reactions and simple versus complex GBC. All these features agree with the concept that the GDME tends to shift the transition state to an earlier step of the cyclization reaction.

Experimental Section

General Procedures. The melting points were measured in capillaries, the IR spectra in CHCl_3 on a Specord IR 75 instrument and the ^1H NMR spectra on a Bruker WM-250 instrument. ^1H -NMR signals were referenced TMS and coupling constants are given in Hz and without sign. Mass spectra EI on a JEOL JMS-D 300 spectrometer. pHs were measured with a Radiometer pH M 84 Research pH-meter using a GK 2401 C electrode. *Materials.* Inorganic reagents and buffer components were of analytical grade and used without further purification. Potassium hydroxide and buffer solutions were prepared with CO_2 -free distilled water.

3-Substituted ethyl 2-methyl-5-(4-nitrophenyl)hydantoates 2b-,2c-,2d-UA. We prepared the starting *N*-substituted alanines^{11,12} using the procedure of Lawson and Morley¹² from 2-bromopropionic acid and the respective amine. After removing carefully all traces of excess amine *in vacuo*, the free amino acids were obtained in pure form by passing through a column packed with ion-exchange resin Amberlite IR-120 in H^+ -form and eluting with 2N ammonia. The solution of the amino acid was evaporated to dryness. Recrystallization from ethanol to gave products with literature m.p. in 76-93% yields. Standard esterification¹³ with HCl/EtOH and

vacuum distillation afforded the amino esters in high yields. The ethyl hydantoates **2b-2d-UE** were prepared from the freshly distilled amino esters and p-nitrophenyl isocyanate according to the procedure described in ref. 2 and used without further purification due to their instability.

1-Substituted-5-methyl-3-(4-nitrophenyl)hydantoins 2b-,2c-,2d-Hyd. The product hydantoins **2b-2d-Hyd** were prepared from the respective amino acids and p-nitrophenyl isocyanate as detailed in ref. 2. The compounds were recrystallized from ethanol-water 2:1.

The properties of the compounds synthesized are summarized in Tables 5 and 6.

Table 5. Melting-points, yields of syntheses and elemental analyses of ethyl 3-substituted-2-methyl-5-(4-p-nitrophenyl)hydantoates **2-UE** and 1-substituted-5-methyl-3-(4-nitrophenyl)hydantoins **2-Hyd**

Compound	mp. °C	Yield %	ν_{CO} cm ⁻¹	Formula (MW)	M+ m/z	Calculated/found (%) ^a		
						C	H	N
2b-UE	125-126	84	1726 1675	C ₁₄ H ₁₉ N ₃ O ₅ (309.3)	309			
2c-UE	108-109	91	1724 1674	C ₁₅ H ₂₁ N ₃ O ₅ (323.3)	323			
2d-UE	118-120	90	1726 1673	C ₁₈ H ₂₅ N ₃ O ₅ (363.2)	363			
2b-Hyd	125-126	74	1775 1720	C ₁₂ H ₁₃ N ₃ O ₄ (263)		54.75 54.44	4.98 4.82	15.92 15.72
2c-Hyd	111-112	65	1770 1715	C ₁₃ H ₁₅ N ₃ O ₄ (267)		56.31 56.43	5.45 5.28	15.15 15.39
2d-Hyd	121-122	52	1770 1722	C ₁₆ H ₁₉ N ₃ O ₄ (345)		60.56 61.04	6.03 5.86	13.24 13.18

^a Calculated values in first row, found values in second row.

Table 6. ¹H NMR spectra of ureido esters and hydantoins in CDCl₃, δ in ppm from TMS, couplings^a in Hz

Compound	2-H	2-CH ₃	N-R		NH	<i>o</i> -H ^b	<i>m</i> -H ^b
2b-UE^c	4.622q (7.3)	1.543d (7.3)	CH ₂	CH ₃	7.391s	7.555d (9.2)	8.186d (9.2)
			3.450m ^d	1.299t (7.2)			
2b-Hyd	4.180q (7.0)	1.571d (7.0)	3.312 ^e (7.2, 14.1)	1.272 (7.2)		7.783d (9.2)	8.312d (9.2)
			3.900 ^e				

(7.2, 14.1)							
2c-UE^f	4.066q (7.3)	1.585d (7.3)	CH 4.445 ^g (6.8)	CH ₃ 1.235d (6.8) 1.251d (6.7)	8.478s	7.544d (9.2)	8.161d (9.2)
2c-Hyd	4.175q (6.9)	1.612d (6.9)	4.230 ^g (6.9)	1.390d (6.9) 1.401d (6.9)		7.783 (9.2)	8.308d (9.2)
2d-UE^h	4.092q (7.3)	1.571d (7.3)	CH(C ₅ H ₁₀) 3.994 ⁱ	C ₅ H ₁₀ 1.08-1.88	8.475s	7.545d (9.2)	8.161d (9.2)
2d-Hyd	4.174q (6.9)	1.613d (6.9)	3.792 ^{tt} (12.0, 3.9)	1.10-2.00		7.780d (9.2)	8.312d (9.2)

^a In parenthesis. ^b Signals show additional fine structure. ^c OCH₂ 4.231q (7.1); OCH₂CH₃ 1.303t(7.1). ^dDue to small chemical shift difference of the two diastereotopic protons. ^e Sextet. ^f OCH₂ 4.262 m due to different chemical shifts of methylene protons, OCH₂CH₃ 1.3093t (7.1). ^g Septet. ^h OCH₂ 4.267 m due to different chemical shifts of methylene protons, OCH₂CH₃ 1.306t (7.1). ⁱPoorly resolved triplet of triplets (11, 3).

Product analysis. The cyclizations of the ethyl hydantoates studied in this paper proceeded quantitatively to the corresponding hydantoins. Good isosbestic points were obtained for all three compounds studied and the end-point absorbances for the kinetic runs were identical within experimental error with the absorbances of model solutions of the respective hydantoins.

Kinetic measurements. Rate constants were determined at (25.0 ± 0.01) °C under pseudo-first order conditions in the thermostatted cell compartment of a Unicam SP-800 or Carl Zeiss Jena UV VIS spectrophotometer. The rates of cyclization of the substituted esters were followed by monitoring the decrease of the absorbance at 330 nm due to the 4-nitrophenylureido group.

Reactions were initiated by injecting 20 μL of 1x10⁻² M stock solutions of the substrates in dry THF into 2.7 cm³ preheated buffer solution. Ionic strength was maintained constant (1.0 M) with KCl. Pseudo-first-order rate constants[§], *k*_{obs}, were obtained by nonlinear-regression curve fitting to the equation $A_t = A_0 e^{-k_{\text{obs}}t} + A_\infty$ by means of the GRAFIT program where *A*_t, *A*₀, and *A*_∞ are the absorbances at times *t*, zero, and infinity, respectively.

pH-Values were measured at the end of each kinetic run. No interference from ester hydrolysis was detected as judged by the good linear plots (*r* > 0.999) of ln(*A*_t - *A*_∞) against time obtained over three half-lives.

The individual rate constants were obtained also by means nonlinear regression fitting to the respective rate equations by means of the GRAFIT program.

Acknowledgements

Helpful discussions with Dr. B. I. Blagoeva are gratefully acknowledged.

References

1. (a) Ingold, C. K. *J. Chem. Soc.* **1921**, 119, 305. (b) Ingold, C. K.; Sako, S.; Thorpe J. F. *J. Chem. Soc.* **1922**, 1117. (c) Allinger, N. L.; Zalkow, V. *J. Org. Chem.* **1960**, 25, 701. (d) Blagoeva, I. B.; Kurtev, B. J.; Pojarlieff, I. G. *J. Chem. Soc., Perkin Trans. 2* **1979**, 1115. (e) Kirby, A. J. *Adv. Phys. Org. Chem.* **1980**, 17, 183. (f) Valter, R. E. *Usp. Khim.* **1982**, 51, 1374. (g) Mandolini, L. *Adv. Phys. Org. Chem.* **1986**, 22, 17. (h) Verevkin, S. P.; Kümmerlin, M.; Beckhaus, H.-D.; Galli, C.; Rüchardt, C. *Eur. J. Org. Chem.* **1998**, 579.
2. Blagoeva, I. B.; Kirby, A. J.; Koedjnikov, A. H.; Pojarlieff, I. G. *Can. J. Chem.* **1999**, 77, 849.
3. Atay, E.; Blagoeva, I. B.; Kirby, A. J.; Pojarlieff, I. G. *J. Chem. Soc., Perkin Trans. 2* **1998**, 2289.
4. Koedjnikov, A. H.; Blagoeva, I. B.; Pojarlieff, I. G.; Kirby, A. J. *J. Chem. Soc., Perkin Trans. 2* **1996**, 2479.
5. Kaneti, J.; Kirby, A. J.; Koedjnikov, A. H.; Pojarlieff, I. G. unpublished results.
6. Davies K.J.; Page, M.I. *J. Chem. Soc., Chem. Commun.* **1990**, 1448.
7. Jencks, W.P. *Acc. Chem. Res.* **1976**, 9, 425.
8. Blagoeva, I. B.; Kirby, A. J.; Kochiyashki, I. I.; Koedjnikov, A. H.; Pojarlieff, I. G.; Toteva, M. M. *J. Chem. Soc. Perkin Trans. 2*, **2000**, 1953
9. Detar, D. F.; *J. Am. Chem. Soc.* **1982**, 104, 7205.
10. Blagoeva, I.B. *J. Chem. Soc., Perkin Trans. 2* **1987**, 127.
11. Skita, A.; Wulff, C. *Ann.* **1927**.
12. Lawson, A. C.; Morley, M. V. *J. Chem. Soc.* **1955**, 453, 190.
13. Leonard, N. J.; Rnyle, W. V. *J. Am. Chem. Soc.* **1949**, 71, 3094.
14. (a) Allinger, N. L.; Yuh, Y. H.; Lii, J. H. *J. Am. Chem. Soc.* **1989**, 111, 8551. (b) Lii, J. H.; Allinger, N. L. *J. Am. Chem. Soc.* **1989**, 111, 8566. (c) Lii, J. H.; Allinger, N. L. *J. Am. Chem. Soc.* **1989**, 111, 8576. (d) MM3 (92), Technical Utility Corporation, 235 Glen Village Court, Powell, OH 43065.
15. Stewart, J. J. P. MOPAC 93.00, Fujitsu Ltd., Tokyo, Japan, 1993.